J. Phys.: Condens. Matter **22** (2010) 285101 (7pp) doi:10.1088/0953-8984/22/28/285101

Linking rigidity transitions with enthalpic changes at the glass transition and fragility: insight from a simple oscillator model

Matthieu Micoulaut

Laboratoire de Physique Théorique de la Matière Condensée, UPMC—Université Paris 6, CNRS UMR 7600, Boite 121, 4 place Jussieu, F-75252 Paris Cedex 05, France

Received 29 March 2010, in final form 11 May 2010
Published 15 June 2010
Online at stacks.iop.org/JPhysCM/22/285101

Abstract

A low temperature Monte Carlo dynamics of a Keating-like oscillator model is used to study the relationship between the nature of network glasses from the viewpoint of rigidity, the thermal reversibility during the glass transition and the strong–fragile behaviour of glass-forming liquids. The model shows that a Phillips optimal glass formation with minimal enthalpic changes is obtained under a cooling/annealing cycle when the system is optimally constrained by the harmonic interactions, i.e. when it is isostatically rigid. For these peculiar systems with a nearly reversible glass transition, the computed activation energy for relaxation time shows also a minimum, which demonstrates that isostatically rigid glasses are strong (Arrhenius-like) glass-forming liquids. Experiments on chalcogenide and oxide glass-forming liquids are discussed under this new perspective and confirm the theoretical prediction for chalcogenide network glasses whereas limitations of the approach appear for weakly interacting (non-covalent, ionic) systems.

(Some figures in this article are in colour only in the electronic version)

1. Introduction

The question of the liquid to glass transition in network-forming systems and the nature of its characteristic temperature T_g have received a huge amount of interest in recent years with a special emphasis on the dynamic properties of the glass-forming liquid [1–5]. Thermodynamic studies have been undertaken as well and these usually allow us to determine the glass transition temperature, that is the temperature at which the system is no longer able to equilibrate on experimental timescales. Usually, this quantity therefore depends on the waiting time before the experiment is performed, and on the (constant) scan rate of the differential scanning calorimetry set-up.

The slowing down of the dynamics is mostly tracked from viscosity (or structural relaxation time τ_α measurements). The behaviour of these quantities with temperature not always displays an Arrhenius-like (or strong) behaviour. When properly rescaled with $1/T_g$ in a semi-log plot, the viscosity or relaxation time can indeed display a variety of different behaviours usually quantified by a fragility index M [6], which characterizes the steepness of the slope of the relaxation time near the glass transition:

$$M = \left[\frac{\mathrm{d}\log_{10}\tau_\alpha}{\mathrm{d}\left(\frac{T_g}{T}\right)}\right]_{T=T_g} \tag{1}$$

M ranges typically between 16 for the strong (Arrhenius behaving) silica liquid to $M = 76$ for the fragile ortho-terphenyl which changes its viscosity by ten orders of magnitude over only a 50 K temperature change. One should also note that in the case of an Arrhenius behaviour for the relaxation time with activation energy E_A, one can relate both quantities:

$$M = \frac{E_A}{k_B T_g}\log_{10} 2 \tag{2}$$

where k_B is the Boltzmann constant. There have been various efforts to connect the liquid fragility to some easily measurable quantities in the glassy state such as compressibility [7] or

Poisson ratio [8], or to the out-of-equilibrium behaviour [9]. At a more microscopic level, combined effects of the structure and the local mechanical behaviour arising from the interaction potential have to act on the dynamical and calorimetric behaviour at the glass transition and thus on the fragility. From a theoretical viewpoint, one may therefore wonder how simple (and of course limited) but insightful models can determine the effect of the potential strength in the low temperature glassy state on the enthalpic behaviour close to T_g, and the relaxing behaviour at higher temperatures.

The present paper attempts to address this basic issue by following the Monte Carlo dynamics of a harmonic Keating-like oscillator model that reproduces the elastic features (flexible, isostatic, stressed rigid) of the glass. Glasses are usually considered as exponentially complex [10]. However, in practice a harmonic (or polynomial) approximation is necessary in order to be able to do some exact calculations and recent examples have shown that such approximations could describe quantitatively some specific features in glass science [11]. We follow the same trail in the following.

The solution of the model not only shows that a hysteretic behaviour can be obtained when cycling through the glass transition region, but also shows that isostatic (i.e. optimally constrained or intermediate) glasses exhibit a minimum in the energy change during the cooling–annealing cycle through the glass transition, independently of the applied cooling rate, a result that matches exactly the Phillips optimal glass condition [12]. Furthermore, the present minimum is correlated with the minimum obtained in the activation energy for relaxation (thus the fragility via equation (2)). These findings are discussed and compared with recent experimental data on network glasses. The results are qualitatively similar to experiment, and more elaborate results would require very complex simulations. One can thus conclude that isostatic glasses are reversible and strong glass-forming liquids, a result that opens new perspectives for the description of glass-forming liquids from the viewpoint of the mechanical behaviour of the glass. And, since rigidity can also be tuned in soft solids and colloids [13], it may provide a general clue for an improved understanding of the dynamic properties leading to a strong viscosity behaviour with low fragility.

The elastic nature of network glasses with changing connectivity (or mechanical constraints n_c derived from Lagrange–Maxwell counting [14]) can be modelled in the framework of rigidity theory [15, 16] using a Keating potential that represents a semi-empirical description of covalent bond-stretching (BS) and bond-bending (BB) forces. From this description, it appears that the number of zero frequency (floppy) modes f behaves as $3 - n_c$. The glass composition at which one has the vanishing of f corresponds to the Maxwell–Lagrange isostatic condition $n_c = 3$.

2. Bimodal floppy mode–Keating oscillator model

We consider a network of N atoms with mass m having two types of harmonic oscillators with respective density $f = 3 - n_c$ if $n_c < 3$, otherwise zero, and n_c. The first has a typical frequency ω associated with the harmonic motion due to the floppy modes, i.e. the modes that allow a local distortion of the network with a low cost in energy. The second has a typical frequency Ω and represents the Keating potential containing the constraints imposed by BB and BS forces [17, 18]. A similar approach has been recently used to describe the effect of rigidity on the glass transition temperature [19]. For $n_c < 3$, the interaction potential V is then given by

$$V = e + E = \frac{m}{2} \sum_{i=1}^{N} f\omega^2 x_i^2 + n_c \Omega^2 X_i^2 \tag{3}$$

where ω and Ω represent respectively the floppy mode frequency and a typical vibrational mode related to BS or BB interactions. In the stressed-rigid phase, as $f = 0$, V reduces to the Keating oscillator E.

An inelastic neutron study [20] of the ternary network glass Ge–As–Se provides information about the order of magnitude of the floppy mode, and the typical BS and BB vibrational frequencies (energies). The floppy mode energy is about 4 meV while identified bond-stretching and bond-bending vibrations have a respective energy of 31 and 19 meV, i.e. about six times more than for the floppy mode energy. Thus one has $\Omega \sim 6\omega$ and this ratio will be used for the forthcoming numerical applications.

We now build on the approach developed by Ritort *et al* [21, 22], i.e. an energetic move ΔV is realized on the oscillators. It is applied according to the Metropolis algorithm, i.e. accepted with probability 1 if the energy decreases, otherwise with a probability $\exp(-\beta \Delta V)$.

The positions of the Keating and the floppy mode oscillators are simultaneously shifted to $X_i + R_i/\sqrt{N}$ and $x_i + r_i/\sqrt{N}$, where R_i and r_i are random variables with a Gaussian distribution having zero mean and respective variance Δ^2 and δ^2.

In comparing the nature of both oscillators, one obviously has $\delta \gg \Delta$ as motion around the position x_i is facilitated by floppy modes, whereas the amplitude X_i of the 'Keating' oscillators should be restricted to small displacements, typically a fraction of the interatomic bond distance [23].

The transition probability for the change in energy ΔV is

$$\begin{aligned} P(\Delta V) = & \int_{-\infty}^{\infty} \left(\prod_i \frac{\mathrm{d}R_i}{\sqrt{2\pi\Delta^2}} \exp(-R_i^2/2\Delta^2) \right) \\ & \times \left(\prod_i \frac{\mathrm{d}r_i}{\sqrt{2\pi\delta^2}} \exp(-r_i^2/2\delta^2) \right) \\ & \times \delta \Bigg[\Delta V - \frac{m n_c \Omega^2}{2} \sum_i \left(\frac{X_i R_i}{\sqrt{N}} + \frac{R_i^2}{N} \right) \\ & - \frac{m f \omega^2}{2} \sum_i \left(\frac{x_i r_i}{\sqrt{N}} + \frac{r_i^2}{N} \right) \Bigg]. \end{aligned} \tag{4}$$

Using the Fourier transform representation of the delta function, equation (4) can be expressed as a Gaussian in the limit $N \to \infty$ as

$$P(\Delta V) = \frac{1}{\sqrt{4\pi Q(t)}} \exp\left[-\frac{(\Delta V - V_0)^2}{4Q(t)} \right] \tag{5}$$

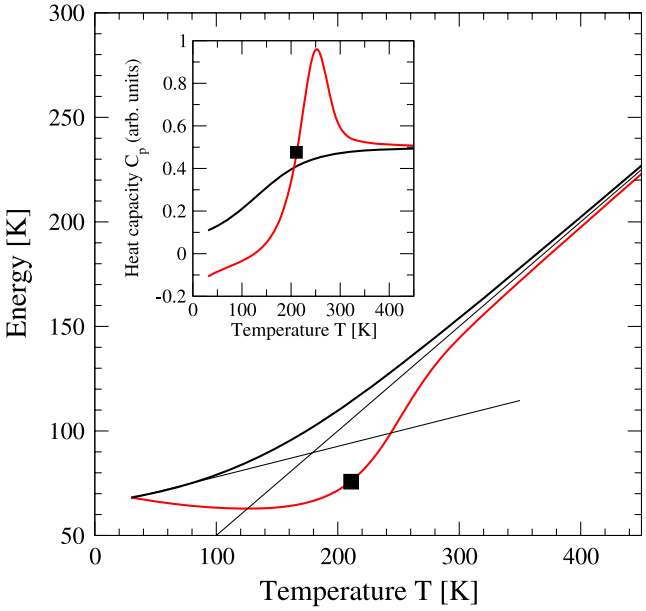

Figure 1. Energy $V(T)$ of a flexible system ($n_c = 2.2$, solution of equation (9)) under cooling (black, upper curve, leading to $V^*(q)$ at low temperature, see the text for details) and annealing (red lower curve) for a rate $q = \pm 1$ K s^{-1}. Linear extrapolations (thin lines) have been drawn to extract an approximate T_g. The inset shows the corresponding heat capacity C_p as a function of temperature and the inflection point of the heating curve serves to define a '*calorimetric*' T_g (filled box) as in the experiment.

with

$$V_0 = \frac{m}{2}[f\omega^2\delta^2 + n_c\Omega^2\Delta^2] \tag{6}$$

and

$$Q(t) = f\omega^2\delta^2\langle e(t)\rangle + n_c\Omega^2\Delta^2\langle E(t)\rangle \tag{7}$$

where t represents the time and the brackets time averages. The mean position of the oscillators have been taken as zero and the time averages performed over different dynamical histories but with the same initial condition for the ensemble.

From the Metropolis rule, one can then write the equation for the evolution of the energy as

$$\tau_0\frac{\partial V}{\partial t} = \int_{-\infty}^{0} x\,P(x)\,\mathrm{d}x + \int_{0}^{\infty} x\,P(x)\mathrm{e}^{-\beta x}\,\mathrm{d}x \tag{8}$$

where τ_0 is a typical time during which the energy change over the oscillators has been performed.

When applied to the probability distribution (5) this leads to

$$\tau_0\frac{\partial V}{\partial t} = \frac{V_0}{2}\left[\left(1 - \frac{2\beta Q(t)}{V_0}\right)g(t) + \mathrm{erfc}\left(\frac{V_0}{2\sqrt{Q(t)}}\right)\right] \tag{9}$$

with erf the complementary error function and

$$g(t) = \exp(-\beta V_0 + \beta^2 Q(t))\mathrm{erfc}\left(\frac{2\beta Q(t) - V_0}{2\sqrt{Q(t)}}\right). \tag{10}$$

Equation (9) is not closed, because it depends on $Q(t)$ through the time dependence of the averages of the floppy mode or constraint energies $e(t)$ and $E(t)$. For simplicity, we solve equation (9) in the low temperature–long time adiabatic approximation [24] where the derivative of the energy V is zero. One then has from equation (9)

$$Q(t) = \frac{T}{2}(2V_0) \cong 2V_0V(t). \tag{11}$$

First, one can solve equation (9) to obtain the behaviour of the energy $V(T)$ by replacing the time variable t by the temperature variable T via $\dot{T} = q\dot{t}/\tau_0$, where q is the cooling/heating rate, the integration being performed from an initial high temperature T_0. In order to highlight the effect of the number of constraints n_c on $V(T)$, we first work at a fixed cooling/heating rate $q = \pm 1$ K s^{-1} and use $T_0 = 500$ K, $\delta = 10\Delta$, $\Omega = 0.3$ and $\tau_0 = 1$ s.

3. Results

Figure 1 represents the cooling and heating behaviour of $V(T)$ for a given n_c. First, one notes that, at high temperature, the energy of the system is equal to $T/2$, which is also the equilibrium solution of equation (9), in agreement with the equipartition theorem. Glassy behaviour (i.e. deviation from the $T/2$ line) onsets at lower temperature, defining a glass transition region around 150 K. In fact, a low energy extrapolation of $V(T)$ crosses the $T/2$ line around this value and T_g can be approximately determined from this cross-over temperature. The low temperature behaviour of equation (9) is given by

$$\tau_0\frac{\partial V}{\partial t} = \frac{V_0}{2}\mathrm{erfc}\left[\sqrt{\frac{V_0}{8V}}\right] - \sqrt{\frac{2VV_0}{\pi}}\exp\left(-\frac{V_0}{8V}\right) \tag{12}$$

which becomes in the long time limit ($V \gg V_0$)

$$q\tau_0\frac{\partial V}{\partial T} = -\sqrt{\frac{32}{\pi V_0}}V^{3/2}\exp\left(-\frac{V_0}{8V}\right) \tag{13}$$

leading after integration to the relationship $V(T)$ of the energy:

$$\sqrt{\frac{2\pi}{V_0}}\left[\mathrm{erf}\sqrt{\frac{V_0}{8V^*(q)}} - \mathrm{erf}\sqrt{\frac{V_0}{8V(T)}}\right] = -\sqrt{\frac{32}{\pi V_0}}\frac{T}{q\tau_0} \tag{14}$$

where $V^*(q)$ is the $T = 0$ limit of the energy, obviously depending on the cooling rate. The intersection of the linear expansion of $V(T)$ at low temperature (see figure 1) with the equilibrium line $T/2$ allows us to obtain an analytical relationship between the glass transition temperature T_g and the cooling rate q, given by

$$q = -\frac{4T_g}{\pi\tau_0\left(\mathrm{erf}\sqrt{\frac{V_0}{4T_g}} - \mathrm{erf}\sqrt{\frac{V_0}{8V^*(q)}}\right)}. \tag{15}$$

Similarly to the experimental procedure consisting of measuring T_g of a glass from the inflection point in heat flow (or heat capacity), one can also determine from the present model a glass transition temperature from the annealing (heating) curve (inset of figure 1).

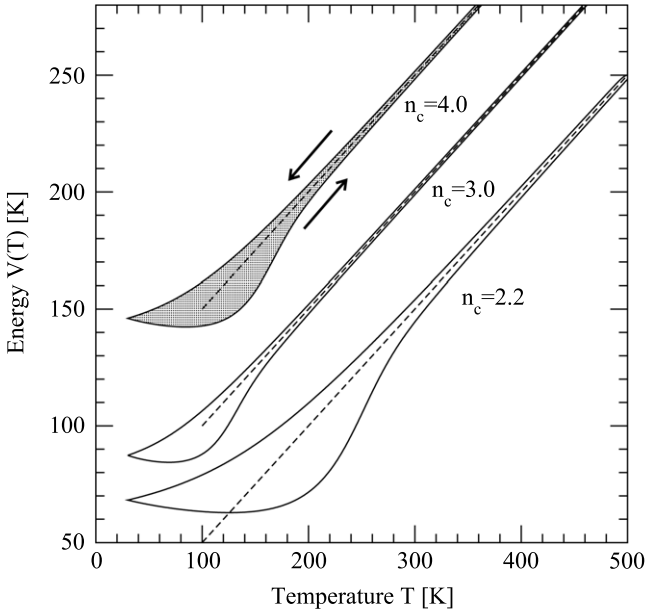

Figure 2. Energy $V(T)$ of the system (solution of equation (9)) under cooling and annealing ($q = \pm 1$ K s^{-1}) for three selected systems: $n_c = 2.2$ (flexible), $n_c = 3.0$ (isostatically rigid) and $n_c = 4.0$ (stressed rigid). The last two curves have been shifted upwards for a clearer presentation. Broken lines represent the equilibrium state $T/2$. The shaded areas (on the curves $n_c = 4$) serve to quantify the enthalpic changes (H) represented in figure 2.

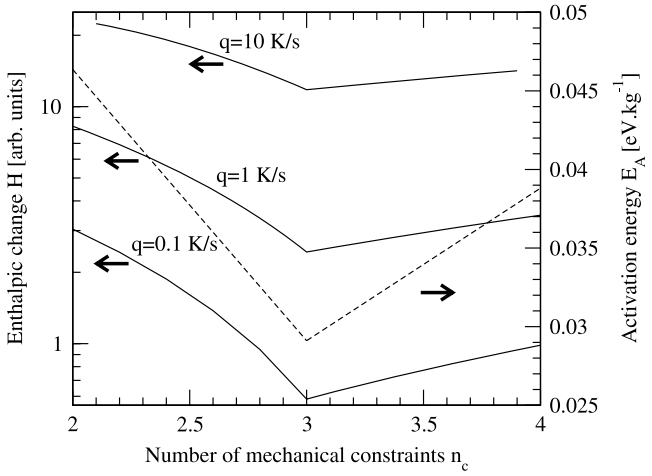

Figure 3. Enthalpic changes H at the glass transition as a function of the number of mechanical constraints n_c for different cycles at cooling/heating rates $q = 0.1$, 1 and 10 K s^{-1}. Right axis: activation energy E_A for relaxation time computed from equation (12).

Annealing from a low temperature end point furthermore shows the typical hysteresis behaviour that is usually manifested in the experiment by an enthalpic overshoot in the heat capacity [25].

From figure 2 representing the evolution of $V(T)$ for three different values of n_c, one sees that the enthalpic change between the cooling and heating curves (quantified by the area) depend on the number of mechanical constraints. Furthermore, these changes are minimized for a system that is nearly isostatically rigid ($n_c = 3$), i.e. when the trial moves can only be realized on the oscillator with the highest frequency Ω. Additional stiffening (i.e. increase of n_c) of the system for $n_c > 3$ leaves the system with a single type of oscillators because $f = 0$ for $n > n_c$, and leads to a global increase of V_0 and thus to an increase of the area as n_c is steadily increased.

The area H defined by the difference between the cooling and heating curves can be tracked with the number of constraints n_c and the corresponding behaviour is displayed in figure 3. It shows that, for a fixed cooling/heating rate q, certain glass transitions occur with minimal enthalpic changes H when cycling through T_g. The model is therefore able to reproduce the Phillips phenomenology of ideal glass formation when a glass is optimally constrained, i.e. isostatic [10, 15]. This is experimentally observed from a characteristic enthalpy ΔH_{nr} (see also figure 4) extracted from complex heat flow measurements at the glass transition [26], which is minimum close to $n_c = 3$.

The study of the dynamics of the system can be achieved from the linearization of equation (9) in the vicinity of the equilibrium value of $V(T)$ that leads to a typical relaxation time:

$$\tau = \frac{\tau_0}{2}\sqrt{\frac{\pi T^3}{V_0^3}}\exp\left[\frac{V_0}{4T}\right]. \qquad (16)$$

The relaxation time is of activated type with an activation energy equal to $E_A = V_0/4$. In figure 3 (right axis) this quantity is represented as a function of the number of mechanical constraints n_c. One can clearly remark that the behaviour of the activation energy for relaxation time (proportional to the fragility, see equation (2)) parallels the enthalpic changes H at the glass transition. A minimum is found for both quantities when the number of floppy modes f vanishes, i.e. when the glass is isostatic, i.e. $n_c = 3$. This point corresponds to the location of the flexible to rigid transition [15] and the centroid of the intermediate phase [25]. We note that the relaxation time is Arrhenius-like and that only a moderate change in fragility can thus be expected from a change in E_A through the variation of the number of constraints. Further inclusions in the potential of equation (2) will be necessary to obtain a Vogel–Fulcher–Tammann law typical of very fragile glass-forming liquids. As we are dealing with harmonic oscillators only (basically vibrations) and neglecting other possible phenomena that may give rise to a VFT behaviour (viscous flow, caging effects, etc), we believe that the model is especially designed for the low temperature behaviour when the dynamics is restricted to harmonic vibrations of the nearly fully connected glass network.

4. Discussion

Is there any experimental evidence highlighting the correlation between isostatic glasses and strong glass-forming liquids? Fairly complete viscosity and calorimetric measurements on several covalent glass-forming liquids are available in the literature. We focus on systems that undergo a flexible to rigid transition, i.e. oxide and chalcogenide glass in selected

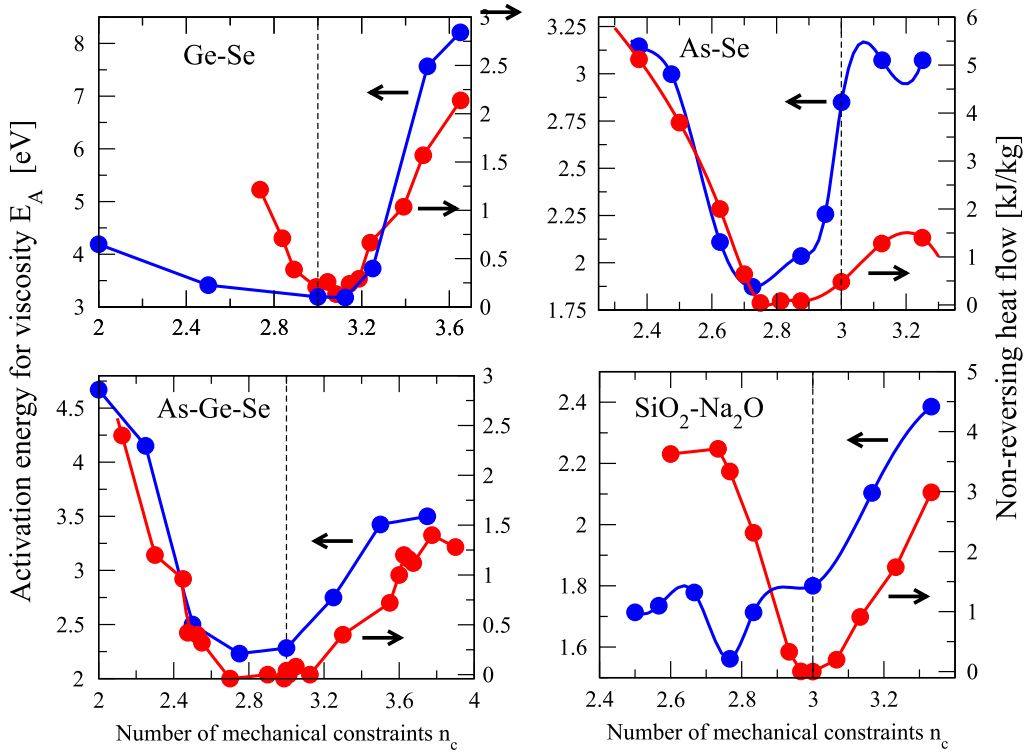

Figure 4. Comparison between the activation energy for viscosity E_A (blue) and the non-reversing heat flow ΔH_{nr} (red) at the glass transition (right axis) as a function of the number of mechanical constraints n_c for four selected glass systems: Ge–Se (data from [27, 28]), As–Se (data from [29, 30]), As–Ge–Se (data from [30, 31]) and sodium silicates (data from [33, 34]). The vertical broken lines indicate the isostatic composition where $n_c = 3$.

composition ranges that lead to a mean coordination number of $\langle r \rangle = 2.4$ and a number of mechanical constraints equal to $n_c = 3$ [10, 15]. Compositional trends in the activation energy for viscosity E_A for binary and ternary chalcogenide and oxide liquids appear in figure 4. In the same figure (right axis) are also projected the non-reversing enthalpies ΔH_{nr} of the corresponding glasses. The latter quantity provides an accurate measure of the enthalpic changes that have taken place during a heating/cooling cycle at the glass transition [25, 26, 29, 30]. One can note that the global minima in the activation energy E_A coincide at $n_c \sim 3$ with those in ΔH_{nr} for chalcogenide glasses. Together with figure 3, these data demonstrate the correlation between the strong–fragile classification of glass-forming liquids with the flexible–intermediate–stressed-rigid classification of the corresponding glasses. The correlation unequivocally shows that intermediate phase glasses, where $n_c \sim 3$, give rise to strong liquids with a low activation energy E_A, while both flexible ($n_c < 3$) and stressed-rigid glasses ($n_c > 3$) give rise to more fragile liquids.

What is the underlying physics governing the relationship? From figure 3, it becomes clear that, when the system is at the rigidity percolation point, temperature-induced structural changes can be accommodated more easily as the energy has decreased because of the decrease, and finally the vanishing, of the floppy mode contribution. On the other hand, the Keating frequency Ω has still not increased due to the progressive stiffening occurring in the stressed-rigid phase.

Chalcogenide glasses can be accurately described with a harmonic Keating potential [10, 23]. Can the present conclusions be extended to glass-forming liquids characterized by more complex potentials different from those shown in equation (3)? The bottom panel of figure 4 already sketches some limitations. In alkali silicate glasses, a large value for n_c corresponds indeed to the silica-rich compositional region, i.e. to systems for which the interaction can be fairly well described by a Keating potential [35]. However, larger amounts of alkali ions (i.e. leading to lower n_cs) increases the number of more weaker (Coulombic) interactions and could cancel the correlation. Weak alkali atom–nonbridging oxygen ionic bonds form, and as $T > T_g$, these weaker interactions cease to act as mechanical constraints enhancing the alkali-atom's mobilities and contributing to the fragility. However, one has to keep in mind that long-range electrostatic interactions may not be that relevant as a short-range mechanical constraint. Still, ionic systems have lower energy barriers towards local atomic arrangements when compared to the high energy cost involved in the breaking of a strong covalent bond, a feature which also implies that the change in electronic configuration between two atoms is small for ionic species. It means that the liquid elasticity length measuring the range of elastic interactions between two relaxational events is small when the temperature is increased [36], leading to a more fragile behaviour for ionic systems. In the modified oxides, one therefore does not expect the glass–liquid correlation to hold as in the chalcogenides. In fact, sodium disilicate and trisilicate are more fragile than SiO_2, even though the trisilicate composition is near the intermediate-phase ($n_c \sim 3$) composition.

An additional counter-example is provided by Trehalose. Recently, constraint counting algorithms have been extended to H-bonded systems [37] and it has been suggested from the structure made of an alternation of weakly and strongly bound glucose rings that Trehalose could represent the case of an optimally constrained network glass. The assumption has been confirmed by calorimetric experiments which have shown that the corresponding non-reversing enthalpy was close to zero [38], i.e. the Trehalose glass belongs to an optimally coordinated network having $n_c \sim 3$. On the other hand, the fragility of liquid Trehalose is rather high [39], $M = 107$, and to reconcile this number with the view at low temperature, weak H-bonds constraining the system must be progressively broken when $T > T_g$. This H-bonded network is therefore an example of an optimally constrained glass that gives rise to a fragile liquid. One can expect a similar circumstance to prevail in all carbohydrates, providing a basis to understand why the fragilities of sugars and alcohols are quite high.

5. Conclusions

In summary, we have shown that a statistical model combining a Keating harmonic potential with a floppy mode oscillator was able to reproduce the generic features of the glass transition from a simple Monte Carlo dynamics: a hysteretic cycle through the glass transition region, a cooling rate dependence of the glass transition temperature and an enthalpic change that depends crucially on the mechanical properties of the glass. Glasses whose structure can be fairly well described by a harmonic potential which are optimally constrained (isostatic) give rise to strong glass-forming liquids, and are found to display glass transitions with few enthalpic changes. Comparison with experiments shows that the demonstrated relationship holds for network glass-forming liquids having strong constraints that are weakly affected by the temperature change. These observations suggest that systems with weaker interactions (e.g. organic glass-forming liquids) will probably not display this kind of relationship.

References

[1] Angell C A 1995 Formation of glasses from liquids and biopolymers *Science* **267** 1924

[2] Gupta P K and Mauro J C 2009 Composition dependence of glass transition temperature and fragility. I. A topological model incorporating temperature-dependent constraints *J. Chem. Phys.* **130** 094503

[3] Trachenko K 2008 The Vogel–Fulcher–Tammann law in the elastic theory of glass transition *J. Non-Cryst. Solids* **354** 3903

[4] Sciortino F 2002 Disordered materials: one liquid, two glasses *Nat. Mater.* **1** 145

[5] Gupta P K and Mauro J C 2008 Two factors governing fragility: stretching exponent and configurational entropy *Phys. Rev.* E **78** 062501

[6] Wang L M, Angell C A and Richert R 2006 Fragility and thermodynamics in nonpolymeric glass-forming liquids *J. Chem. Phys.* **125** 074505

[7] Buchenau U and Wischnewski A 2004 Fragility and compressibility at the glass transition *Phys. Rev.* B **70** 092201

[8] Novikov V N and Sokolov A P 2004 Poisson's ratio and the fragility of glass-forming liquids *Nature* **431** 961
Yannopoulos S N and Johari J P 2006 Poisson's ratio and liquid's fragility *Nature* **442** E7

[9] Mauro J C and Loucks R J 2008 Impact of fragility on enthalpy relaxation in glass *Phys. Rev.* E **78** 021502

[10] Phillips J C 2006 Axiomatic theories of ideal stretched exponential relaxation (SER) *J. Non-Cryst. Solids* **352** 4490

[11] Naumis G G and Flores-Ruiz H M 2008 Low-frequency vibrational mode anomalies and glass transition: thermal stability, phonon scattering, and pressure effects *Phys. Rev.* B **78** 094203

[12] Phillips J C 1979 Topology of covalent non-crystalline solids 1. Short-range order in chalcogenide alloys *J. Non-Cryst. Solids* **34** 153

[13] Wyart M 2005 On the rigidity of amorphous solids *Ann. Phys. Fr.* **30** 1

[14] Lagrange J L 1788 *Mécanique Analytique* Paris
Maxwell J C 1864 *Phil. Mag.* **27** 294

[15] Thorpe M F 1983 Continuous deformations in random networks *J. Non-Cryst. Solids* **57** 355

[16] He H and Thorpe M F 1985 Elastic properties of glasses *Phys. Rev. Lett.* **54** 2107

[17] Wooten F, Winer K and Weaire D 1985 Computer-generation of structural models of amorphous Si and Ge *Phys. Rev. Lett.* **54** 1392

[18] Djordjević B R, Thorpe M F and Wooten F 1995 Computer-model of tetrahedral amorphous diamond *Phys. Rev.* B **52** 5685

[19] Naumis G G 2006 Variation of the glass transition temperature with rigidity and chemical composition *Phys. Rev.* B **73** 172202
Naumis G G 2005 Energy landscape and rigidity *Phys. Rev.* E **71** 026114

[20] Kamitakahara W *et al* 1991 Vibrational densities of states and network rigidity in chalcogenide glasses *Phys. Rev.* B **44** 94

[21] Bonilla L L, Padilla F G and Ritort F 1998 Aging in the linear harmonic oscillator *Physica* A **250** 315

[22] Ritort F 2005 Resonant nonequilibrium temperatures *J. Phys. Chem.* B **109** 6787

[23] Wang R W, Thorpe M F and Mousseau N 1995 Length mismatch in random semiconductor alloys. 4. General multinary compounds *Phys. Rev.* B **52** 17191

[24] Garriga A and Ritort F 2005 Mode-dependent nonequilibrium temperature in aging systems *Phys. Rev.* E **72** 031505

[25] Feng W, Bresser W and Boolchand P 1997 Direct evidence for stiffness threshold in chalcogenide glasses *Phys. Rev. Lett.* **78** 4422

[26] Selvanathan D, Bresser W and Boolchand P 2000 Stiffness transitions in Si_xSe_{1-x} glasses from Raman scattering and temperature-modulated differential scanning calorimetry *Phys. Rev.* B **61** 15061

[27] Wang F, Mamedov S, Boolchand P, Goodman B and Chandrasekhar M 2005 Pressure Raman effects and internal stress in network glasses *Phys. Rev.* B **71** 174201

[28] Stolen S, Grande T and Johnsen H-B 2002 Fragility transition in $GeSe_2$–Se liquids *Phys. Chem. Chem. Phys.* **4** 3396

[29] Borisova Z U 1981 *Glassy Semiconductors* (New York: Plenum)

[30] Georgiev D G, Boolchand P and Micoulaut M 2000 Rigidity transitions and molecular structure of As_xSe_{1-x} glasses *Phys. Rev.* B **62** 9228

[31] Wang Y, Boolchand P and Micoulaut M 2000 Glass structure, rigidity transitions and the intermediate phase in the Ge–As–Se ternary *Europhys. Lett.* **52** 633

[32] Tatsumisago M, Halfpap B L, Green J L, Lindsay S M and Angell C A 1990 Fragility of Ge–As–Se glass-forming liquids in relation to rigidity percolation, and the Kauzmann paradox *Phys. Rev. Lett.* **64** 1549
Böhmer R and Angell C A 1992 Correlations of the nonexponentiality and state dependence of mechanical relaxations with bond connectivity in Ge–As–Se supercooled liquids *Phys. Rev.* B **45** 10091

[33] Bockris J O M, Mackenzie J D and Kitchener J A 1955 Viscous flow in silica and binary liquid silicates *Trans. Faraday Soc.* **51** 1734

[34] Vaills Y, Qu T, Micoulaut M, Chaimbault F and Boolchand P 2005 Direct evidence of rigidity loss and self-organization in silicate glasses *J. Phys.: Condens. Matter* **17** 4889

[35] Galeener F L and Thorpe M F 1983 Rings in central-force network dynamics *Phys. Rev.* B **28** 5802

[36] Trachenko V and Brazhkin V V 2009 Understanding the problem of glass transition on the basis of elastic waves in a liquid *J. Phys.: Condens. Matter* **21** 425104

[37] Phillips J C 2006 Ideally glassy hydrogen-bonded networks *Phys. Rev.* B **73** 024210

[38] Boolchand P, Micoulaut M and Chen P 2008 Nature of glasses *Phase Change Materials: Science and Applications* ed S Raoux and M Wuttig (Heidelberg: Springer) p 37

[39] DeGusseme A, Carpentier L, Willart J F and Descamps M 2003 Molecular mobility in supercooled trehalose *J. Phys. Chem.* B **107** 10879